A Leucine Aminopeptidase-Activated Theranostic Prodrug for Cancer Diagnosis and Chemotherapy

Feiyi Wang,[*,†] *Sisi Hu,*[†] *Qi Sun,*[§] *Qiang Fei,*[#] *Chao Ma,*[†] *Cuifen Lu,*[†] *Junqi Nie,*[†] *Zuxing Chen,*[†] *Jun Ren,*[†] *Guo-Rong Chen,*[‡] *Guichun Yang,*[*,†] *Xiao-Peng He,*[*,‡] *and Tony D James*[*,⊥]

[†] Ministry of Education Key Laboratory for the Synthesis and Application of Organic Functional Molecules & Hubei Collaborative Innovation Center for Advanced Organic Chemical Materials, Hubei University, Wuhan 430062, P. R. China.

[‡] Key Laboratory for Advanced Materials and Institute of Fine Chemicals, Feringa Nobel Prize Scientist Joint Research Center, School of Chemistry and Molecular Engineering, East China University of Science & Technology, Shanghai 200237, P. R. China.

[§] Key Laboratory for Green Chemical Process of Ministry of Education and School of Chemistry and Environmental Engineering, Wuhan Institute of Technology, Wuhan 430205, P. R. China.

[#] Food and Pharmaceutical Engineering Institute, Guiyang University, Guizhou, 550005, P. R. China.

[⊥] Department of Chemistry, University of Bath, Bath, BA2 7AY, UK.

ABSTRACT: Currently chemotherapy is a widely used and important treatment for cancer. However, almost all the treatments have shortcomings associated with poor-specificity and high toxicity, which results in severe side-effects to normal cells and tissue. This is a very important problem yet it currently remains unanswered. Therefore, the development of method for the more effective delivery of anticancer drugs to their targets and real-time monitoring of the drugs localization are very important. Herein, we designed a theranostic prodrug: CPT-*p*-Leu, which was constructed using

fluorescent camptothecin (CPT), a self-immolative linker and leucine (Leu) residue. Upon exposure to LAP (leucine aminopeptidase: LAP), the amide bond in CPT-*p*-Leu will be cleaved, followed by an intramolecular 1, 6-elimination, which triggers the active anticancer drug (CPT) release and recovers the fluorescence of CPT. With our design, the anticancer drug, CPT, can be used as both a drug and a fluorescence reporter, making our system suitable to accurately and effectively track the released CPT distribution. Based on this strategy, CPT-*p*-Leu could achieve the chemoselective detection of LAP and monitoring of the anticancer drug release. Furthermore, it also provides a very convenient way to accurate determine the location of the released drug in living samples. In addition, CPT-*p*-Leu shows good cell membrane permeability and enhanced cytotoxicity toward LAP overexpressing cancer cells. We anticipate that our research will facilitate the development of improved theranostic systems for cancer therapy.

KEYWORDS: Leucine aminopeptidase, Sensor, Theranostic prodrugs, chemotherapy, Bioimaging.

INTRODUCTION

Cancer is a significant life-threatening disease to humans. Currently, the treatment of cancer is focused on chemotherapy, surgery and radiotherapy.[1-4] Chemotherapy, which is one of the most commonly used treatments, is hindered by unwanted and adverse side-effects, such as nausea and vomiting, hair loss, organ damage, and weakening of immune system, due to indiscriminate destruction of both cancerous and normal cells.[5-8] Therefore, the development of systems, that can be precisely activated at the tumor site by the unique tumor microenvironment, such as high glutathione concentations, lower pH values, high ROSs levels and overexpression of enzymes etc.,[9-24] provide a promising strategy to enhance the selectivity and significantly enhance the therapeutic efficiency of drugs towards cancer

cells.

Theranostic prodrugs, diagnostic systems combined with therapeautics have emerged as important treatments for diseases.[25-34] In particular, theranostic prodrugs decorated with fluorophores hold the promise to monitor drug release by fluorescence.[35-40] These kinds of theranostic prodrugs provide significant benefit enabling the behavior of prodrugs to be monitored.

To date, various theranostic prodrug systems have been designed and synthesized.[41-43] However, they are primarily focused on monitoring drug release. In such systems, the fluorophore can report whether the drug is released, but, it is difficult if not impossible to say exactly where the drug is located. Therefore, it is important to monitor both the process of drug release as well as the released drug cellular distribution. Because, therapeutic efficiency is closely associated with the concentration of antitumor drugs in cancerous tissues.

Leucine aminopeptidase (LAP), a key proteolytic enzyme, exists widely in mammals, plants, microbes and cancer cells, catalyzes the hydrolysis of N-terminal leucine residues from protein or peptide substrates, and plays a crucial role in various pathological and physiological processes.[42] A number of reports have indicated that LAP levels can are enhanced in various kinds of tumors, including ovarian epithelial malignancy and breast carcinomas, etc.[45-47] Until now, LAP has been used as an important trigger to activate fluorescence changes in various chemosensors.[48-54] As far as we are aware, no LAP triggered theranostic prodrug systems have previously been reported.

Recently, Wu et al. reported a DT-diaphorase-activatable theranostic prodrug for the specific recognition of DT-diaphorase and monitoring drug release.[19] Inspired by this strategy, herein, we present a LAP-activated theranostic prodrug, CPT-*p*-Leu, which contains an anti-cancer drug, camptothecin (CPT, topoisomerase I inhibitor), a cleavable and self-immolative linker, and leucine

(Scheme 1a). In this theranostic prodrug, CPT, has two roles: First, it serves as a fluorogenic reporter for monitoring LAP because its fluorescence is significantly quenched by the carbonate bond. However, upon LAP enzymatic cleavage of the amide bond, fluorescent CPT is released after an intramolecular 1, 6-self-elimination.[55] Secondly, CPT an anticancer drug can kill cancer cells. Therefore, in our design the fluorescent CPT, drug can be used to accurately visualize the anticancer drugs cellular distribution, and provide location information to help improve therapeutic efficiency (Scheme 1b). As far as we are aware, CPT-*p*-Leu represents the first LAP-activated theranostic prodrug that can monitor LAP activity, report the release of the anticancer drug, and visualize the drug distribution. Resulting in a system that can precisely destroy cancer cells overexpressing LAP with potentially reduced side-effects.

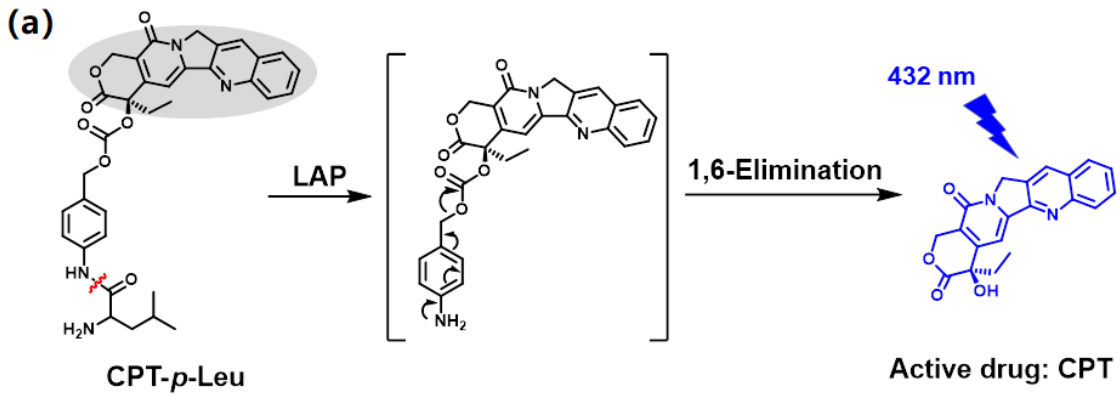

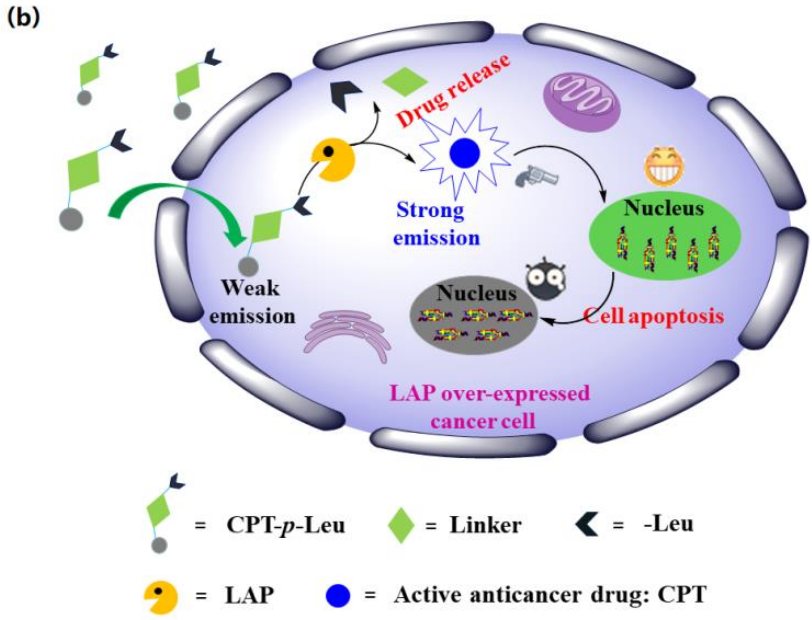

Scheme 1. (a) CPT-*p*-Leu and the proposed mechanism of LAP triggering the fluorescence change and drug release. (b) Schematic illustration of drug release and action in cancer cells.

EXPERIMENTAL SECTION

Chemicals and Instruments: Unless specifically stated, chemical reagents and solvents were used as received from commercial sources. 1-Hydroxybenzotriazole (HOBt), 4-dimethylaminopyridine (DMAP), 2-Propanamine (DIPEA), 1-(3-Dimethylaminopropyl)-3-ethylcarbodiimidehydrochloride (EDC·HCl), Tetrabutylammonium fluoride (TBAF), triphosgene, camptothecin (CPT), Bismuthtrichlorie ($BiCl_3$), Boc-Leu-OH, chloride salts of metal ions (K^+, Ca^{2+}, Zn^{2+}) were purchaused from Aladdin Reagents, Propidium iodide (Pi) was purchased from Tansoole. Leucine aminopeptidase (LAP), glutamyl transpeptidase (GGT), glutathione (GSH), cysteine (Cys), elastase (ELA), α-chymotrypsin (α-Chy), tyrosinase (Tyr), glucoamylase, cellulase, lipase, α-amylase, aprotinin, and sulfatase were purchased from Sigma-Aldrich. Dichloromethane (DCM) and N, N-dimethylformamide (DMF) both dried with calcium hydride (CaH_2) and then distilled under nitrogen

(N_2). Ultrapure water was used in all tests. Column chromatography (silica gel (200-300 mesh)) was used for purification. ^{1}H-NMR and ^{13}C-NMR spectra in DMSO-d_6 or $CDCl_3$ were measured on a Bruker AV-400 NMR spectrometer. High resolution mass spectra (HRMS) were performed on an Agilent 1100 Series. UV-vis absorption and fluorescence spectra were recorded on a SHIMADZU UV1800 and Agilent Cary Eclipse Fluorescence spectrophotometer. High performance liquid chromatography (HPLC) were measured on the Dionex Ultimate 3000. The pH was determined using a METTLER TOLEDO FiveEasy Plus digital pH meter.

General Optical Measurements: For in vitro measurements, CPT-*p*-Leu was first dissolved in dimethyl sulfoxide (DMSO) to prepare a parent stock solution (5.0 mM). Then an appropriate volume of stock solution was diluted to the desired concentration in a quartz cuvette (path length 1 cm) with PBS buffer for optical measurements. The relevant parameters for the measurements of fluorescence are as follow: the excitation wavelength was 350 nm, and slit widths: 5 nm/5 nm.

Cell Cultures and Viability Assay: HeLa cells, A549 cells and HEK 293 cells were grown in a cell culture flask at 37 °C under a humidified 5% CO_2/95% air incubator in Dulbecco's modified Eagle's medium (DMEM) which were supplemented with 10% fetal bovine serum (FBS) and penicillin−streptomycin (0.5 U·mL^{-1} of penicillin and 0.5·g mL^{-1} streptomycin). The cells (A549 cells and HEK293 cells) viability with CPT-*p*-Leu or CPT were evaluated using an MTT assay.[19] For each independent experiment, the assays were repeated five times.

Fluorescent confocal image of cells: Cells were seeded in a glass bottom dish with complete culture medium for 24 h before the experiments. Then cells were loaded with CPT-*p*-Leu or Pi (Propidium iodide) for different times in the culture medium at 37 °C. After treatment, fluorescence imaging was carried out using an Olympus FV1000-MP. The excitation wavelength were 405 nm and 561 nm,

images were collected at 425-470 nm and 590 nm-650 nm for blue channel and red channel, respectively.

RESULTS AND DISCUSSION

CPT-*p*-Leu was synthesized as depicted in Scheme S1. The intermediates and the prodrug were confirmed by ^{1}H NMR and ^{13}C NMR, and high-resolution mass spectrometry (HRMS) (Figure S1-12).

First, the optical properties of CPT-*p*-Leu and CPT were recorded. They both exhibited two absorption bands at 350 nm and 365 nm. With excitation at 350 nm, both of them possess an emission band at 432 nm, while the fluorescence of CPT-*p*-Leu is much weaker (Figure S13 and Table S1). These results reveal that the fluorescence of CPT is significantly reduced by the covalently attached group, and the fluorescence can be restored by cleavage of that group.

Sensing Properties and Proposed Mechanism of LAP toward CPT-*p*-Leu. To confirm that LAP can cleave the amide bond in CPT-*p*-Leu and activate CPT fluorescence *via* an intramolecular 1, 6-self-elimination. The optical properties of CPT-*p*-Leu in the presence of LAP under physiological conditions (PBS buffer solution, 10 mM, pH 7.4, 37 °C) was monitored. As depicted in Figure 1a, CPT-*p*-Leu exhibited weak fluorescence centered at 432 nm, while after treatment with LAP (0.07 U·mL^{-1}), the fluorescence intensity increased gradually more than 5-fold and reached a plateau after 30 min (Figure 1c). At this point the fluorescence spectra was identical to the emission spectrum of the reference CPT (Figure S13b). Moreover, in order to confirm that LAP triggered the anticancer drug (CPT) release from CPT-*p*-Leu, HPLC and HRMS analysis were conducted. As shown in Figure S14, the retention time of pure CPT-*p*-Leu was found to be at 4.61 min. However, after treatment with LAP (0.07 U·mL^{-1}) for 5 minutes, a new product exhibiting a chromatographic peak at 5.95 min was

detected, which was very close to the retention time of pure CPT. Whilst, HRMS analysis of the reaction system indicated that, Leu, CPT and CPT-*p*-Leu could be observed at m/z 132.10187, 349.18371 and 633.23352, respectively. These results demonstrated that CPT-*p*-Leu can serve as a fluorescent probe for tracking LAP activity and monitoring CPT release.

Enzyme Kinetic Parameters of CPT-*p*-Leu. To further investigate the capability of LAP to facilitate anti-cancer drug release from CPT-*p*-Leu, the gradual addition of LAP 0-0.1 $U \cdot mL^{-1}$ to a solution of CPT-*p*-Leu was monitored (Figure 1b). The fluorescence intensity of CPT-*p*-Leu increased steadily until it reached saturation at about 0.07 $U \cdot mL^{-1}$ LAP, suggesting that 0.07 $U \cdot mL^{-1}$ LAP can efficiently catalyze the hydrolysis of 10 μM CPT-*p*-Leu. Likewise, when different concentrations of CPT-*p*-Leu were systematically treated with 0.07 $U \cdot mL^{-1}$ LAP (Figure 1d), a dose-dependent fluorescence increase was observed, and 10 μM CPT-*p*-Leu was sufficient to saturate 0.07 $U \cdot mL^{-1}$ LAP. These phenomena demonstrate that 0.07 $U \cdot mL^{-1}$ LAP and 10 μM CPT-*p*-Leu are the optimal amounts, to trigger anti-cancer drug release in cancer cells in a dose-dependent manner. Moreover, the kinetic values of CPT-*p*-Leu against LAP were also determined using the Michaelis-Menten equation,[48] the Michaelis constant (K_m) of the prodrug was estimated to be 54.02 μM, and the maximum velocity (V_{max}) values was 13.38 $\mu M \cdot min^{-1}$, which indicates that CPT-*p*-Leu has an excellent affinity for LAP.

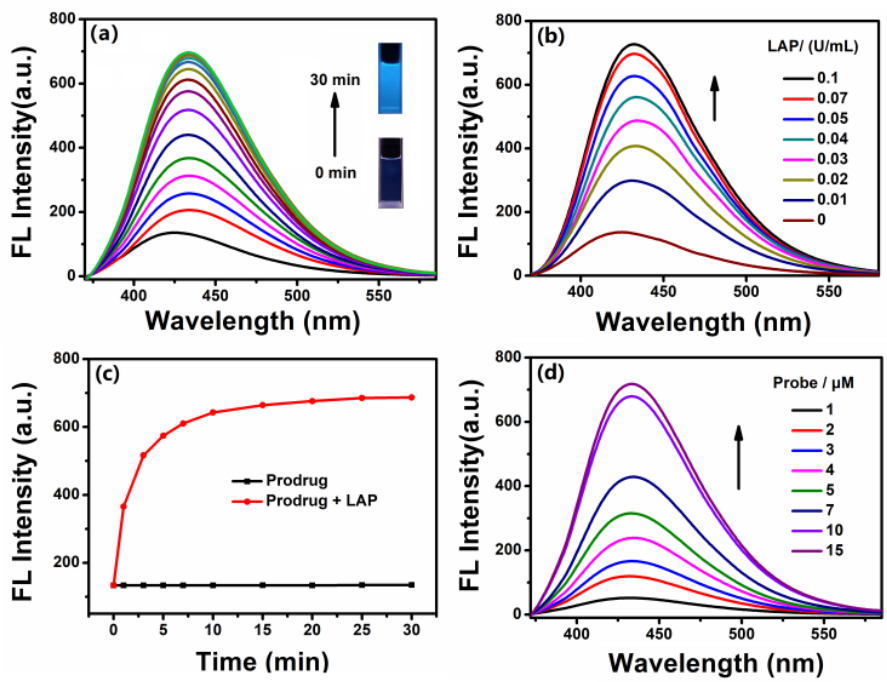

Figure 1. (a) Time-dependent fluorescence spectra of CPT-*p*-Leu (10 μM) upon treatment with LAP (0.07 $U \cdot mL^{-1}$). Inset: photo of CPT-*p*-Leu solution before and after treatment with LAP. (b) Fluorescence spectra of CPT-*p*-Leu (10 μM) incubated with various concentrations of LAP (0, 0.01, 0.02, 0.03, 0.04, 0.05, 0.07, 0.1 $U \cdot mL^{-1}$, respectively) for 30 min. (c) Time-dependence fluorescence intensity at 432 nm for CPT-*p*-Leu (10 μM) treatment with (red) or without (black) of LAP (0.07 $U \cdot mL^{-1}$). (d) The emission spectra of different concentration of CPT-*p*-Leu incubated with LAP (0.07 $U \cdot mL^{-1}$) for 30 min. λ_{ex} = 350 nm.

pH Effect. The pH effect on the drug release of CPT-p-Leu was also evaluated. As illustrated in Figure S15, in the absence of LAP, the fluorescence intensity at 432 nm for CPT-*p*-Leu is stable over a pH range from 5 to 9. Whilst in the presence of LAP CPT-*p*-Leu has a good response to LAP over a pH range from 5 to 9. These observations indicate that our prodrug (CPT-*p*-Leu) is a potential theranostic agent suitable for delivering anticancer drugs to cancer tissues over a biological pH range.

Selectivity of CPT-*p*-Leu. Subsequently, the performance of CPT-*p*-Leu with other biological

relevant analytes was evaluated. To verify CPT-*p*-Leu possess a high specificity to LAP, the prodrug was incubated with various metal ions, biological reductants, and several kinds of enzymes. However, as can be seen from Figure 2, only LAP triggers a fluorescence increase and no significant fluorescence response was observed with other analytes. These results demonstrate that CPT-*p*-Leu can selectively react with LAP in a cellular environment.

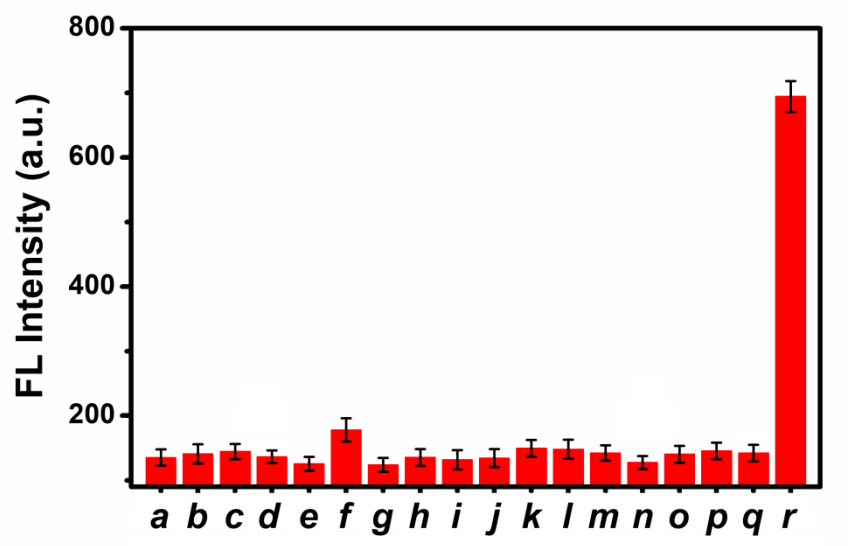

Figure 2. Fluorescence responses of CPT-*p*-Leu (10 μM) treatment with LAP and other analytes in aqueous solution (PBS, 10 mM, pH 7.4) for 30 min, λ_{ex} = 350 nm. Labels: *a*: free; *b*: K^+; *c*: Zn^{2+}; *d*: Ca^{2+}; *e*: HS^-; *f*: GSH; *g*: Cys; *h*: glucoamylase; *i*: cellulase; *j*: lipase; *k*: α-amylase; *l*: aprotinin; *m*: sulfatase; *n*: Tyr; *o*: ELA; *p*: α-Chy; q: GGT; r: LAP. Error bars represent standard deviation of three independent experiments.

Live Cell Imaging. Based on these observations where LAP can trigger anticancer drug release with concurrent fluorescence activation, CPT-*p*-Leu was evaluated in cells. HeLa cells were first utilized for evaluating the cellular uptake and fluorescence intensity changes. The fluorescence confocal imaging results are illustrated in Figure 3, free HeLa cells show negligible fluorescence in the blue

channel. Whilst after 30 min incubation with CPT-*p*-Leu, a strong fluorescence signal was observed. Furthermore, in order to confirm the fluorescent signal was caused by LAP, inhibitor experiments were conducted. Firstly, HeLa cells were pretreated with inobestin (a LAP inhibitor) for 30 min, and then CPT-*p*-Leu was added, and the system was further incubated for another 30 min. As shown in Figure 3h and j, the fluorescence intensity was significantly suppressed by inobestin.

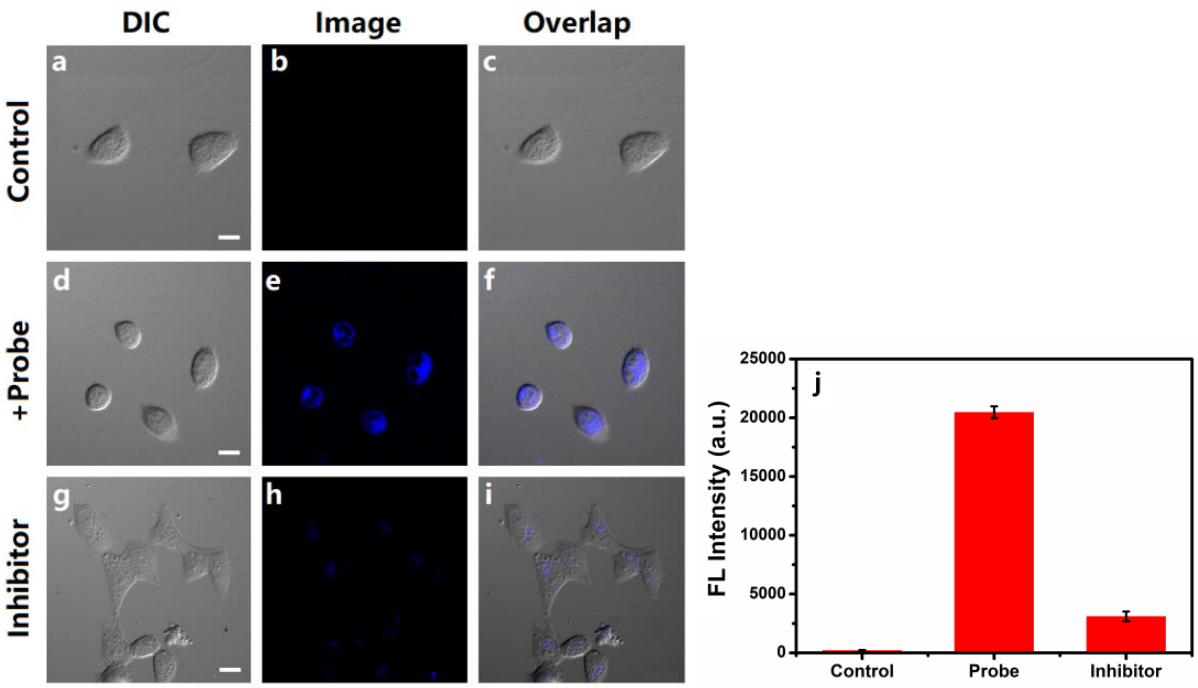

Figure 3. Confocal images of HeLa cells in the absence (a-c) or presence (d-f) of CPT-*p*-Leu (10 μM) for 30 min. For the inhibition experiment (g-i), HeLa cells were pretreated with inobestin (50 μM) for 30 min and then CPT-*p*-Leu (10 μM) was added and further incubated for another 30 min. (a, d, g) DIC images, (b, e, h) FITC channels (425 nm- 470 nm), (c, f, i) overlapped images. (j) Average fluorescence intensity. Error bars represent standard deviation of three independent experiments. Scale bars = 20 μm.

In addition, in order to confirm that CPT-*p*-Leu is selectively activated in LAP overexpressing cancer

cells but not in normal cells, a series of control cell imaging assays were carried out using HEK 293 cells as the control. As shown in Figure S16 and S17, a significantly brighter fluorescence was observed in A549 cells compared to the control cells, which suggests that CPT was released more in the cancer cells. Moreover, we monitored the process of drug release and drug distribution in A549 cells with fluorescence microscopy. As shown in Figure 4, with increasing incubation time, CPT was gradually released to the cytoplasm, followed by entry into the nucleus, as determined by fluorescence co-localization with a nucleus tracker (Pi: Propidium iodide). These results demonstrated that the fluorescence enhancement was caused by LAP in cancer cells. At the same time, the anticancer drug, CPT, was released and the fluorescence signal distribution in these cells indicated the drug localization.

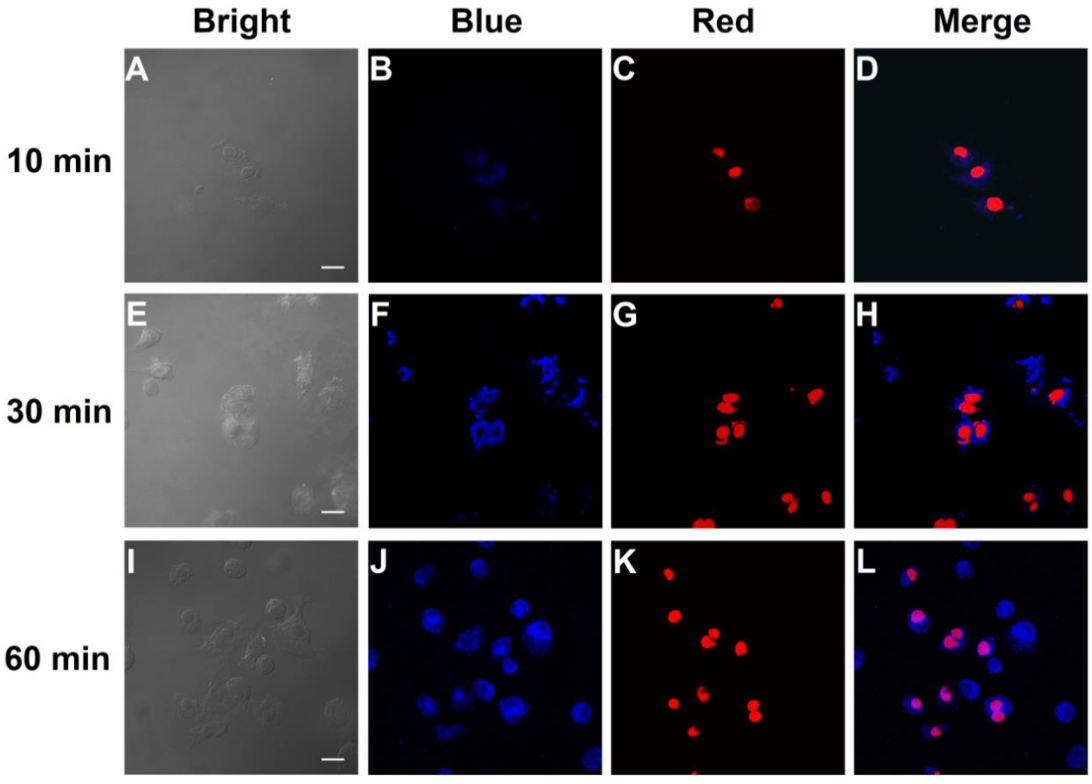

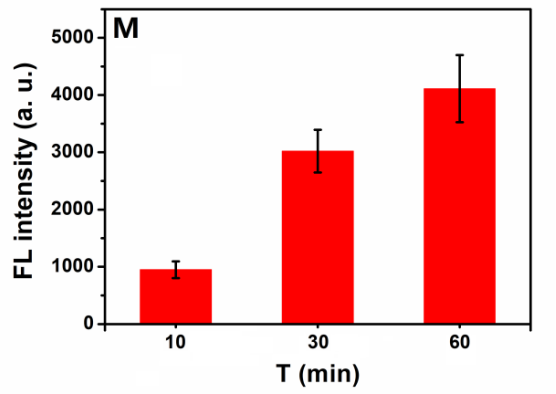

Figure 4. Confocal images of A549 cells. Cells were treated with 10 μM prodrug for (A-D) 10 min, (E-H) 30 min, and (I-L) 60 min, then the cells were co-stained with Nuclei-Tracker (Pi: red). (A, E, I) DIC images, (B, F, J) blue channel (425 nm- 470 nm), (C, G, K) red channel (590 nm- 650 nm), (D, H, L) merged images. (M) Average fluorescence intensity in blue channel. Error bars represent standard deviation of three independent experiments. Scale bars = 20 μm.

Subsequently, cell viability experiments were carried out to assess CPT-*p*-Leu cytotoxicity towards LAP overexpressing cancer cells (A549) and normal cells (HEK 293) using typical MTT assays. As shown in Figure 5, CPT-*p*-Leu displays relatively strong cytotoxicity towards A549 cells, and the cell viability was under 40% when incubated with the prodrug at 20 μM for 24 h. However, cytotoxicity was significantly lower for the non-LAP overexpressing normal cell, HEK 293, and the cell viability was over 70% when treated under the same conditions. These results indicated that CPT-*p*-Leu can selectivity harm LAP overexpressing cancer cells.

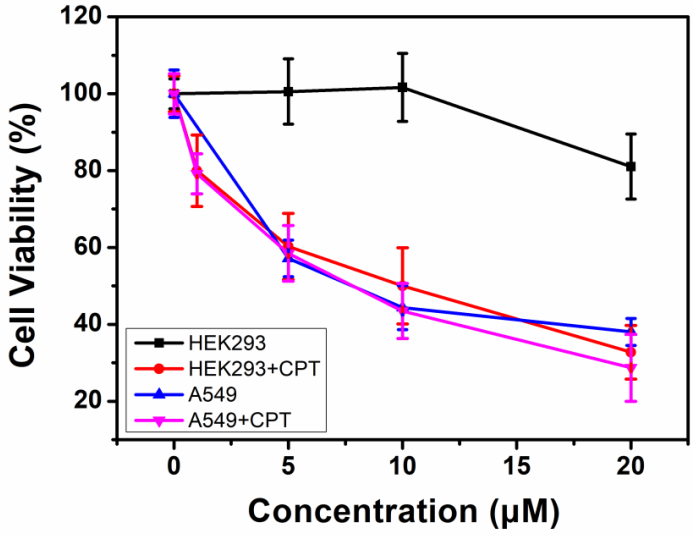

Figure 5. Cell viability of HEK 293 and A549 cell lines incubated with CPT-*p*-Leu and CPT at various concentrations for 24 h. Error bars represent standard deviation of five independent experiments.

CONCLUSION

In this study, a new LAP-activatable theranostic prodrug, CPT-*p*-Leu, was developed. Upon interaction with LAP, the cleavage of the amide bond in CPT-*p*-Leu is facilitated followed by an intramolecular 1, 6-elimination, which triggers release of the active anticancer drug (CPT) and restores the fluorescence of CPT. Therefore, CPT-*p*-Leu can be used for the chemoselective detection of LAP and real-time monitoring of anticancer drug release. Furthermore, the anti-cancer drug CPT, serves as the reporter, and allows accurate determination of the location of the released drug in living samples. In addition, CPT-*p*-Leu shows good cell membrane permeability and enhanced cytotoxicity toward LAP overexpressing cancer cells. We anticipate that our strategy of using anti-cancer drugs, which serve as both a bioactive molecule and the signal reporter, make these systems suitable for the accurate and effective real-time tracking of released drugs. Which will help provide useful insight for the

development of future theranostic systems for cancer diagnosis and treatment. In addition, we anticipate that our work will help provide guidance in the development of new and improved theranostic systems for cancer therapy.

ASSOCIATED CONTENT

Supporting Information

Details of organic synthesis, compounds characterization, HPLC analysis, supplementary optical spectra, additional cell images, and additional references. The Supporting Information is available free of charge on the ACS Publications website.

AUTHOR INFORMATION

Corresponding Authors:

* Email: yangguichun@hubu.edu.cn

* Email: wangfyi@hubu.edu.cn

* Email: xphe@ecust.edu.cn

* Email: t.d.james@bath.ac.uk

Notes

The authors declare no competing financial interest.

ACKNOWLEDGMENT

This research work was supported by the National Natural Science Foundation of China (21702053, 21676075, 51603064, 21804102 and 21776078), the National Key Research and Development Program of China (2016YFA0101100), the Guizhou Provincial Department of Science and

Technology Foundation project ([2019]1015). TDJ wishes to thank the Royal Society for a Wolfson Research Merit Award.

REFERENCES

1. Chambers, A. F.; Groom, A. C.; MacDonald, I. C. Dissemination and growth of cancer cells in metastatic sites. *Nat. Rev. Cancer* **2002**, *2*, 563-572.
2. Hortobagyi, G. N.; Ames, F. C.; Buzdar, A. U.; Kau RN, S. W.; McNeese, M. D.; Paulus, D.; Hug, V.; Holmes, F. A.; Romsdahl, M. M.; Fraschini, G.; McBride, C. M.; Martin, R. G. and Montague, E. Management of stage III primary breast cancer with primary chemotherapy, surgery, and radiation therapy. *Cancer* **1988**, *62*, 2507-2516.
3. Lotfi-Jam, K.; Carey, M.; Jefford, M.; Schofield, P.; Charleson, C. and Aranda, S. Nonpharmacologic strategies for managing common chemotherapy adverse effects: a systematic review. *J. Clin. Oncol.* **2008**, *26*, 5618-5629.
4. Herskovic, A.; Martz, K.; Al-Sarraf, M.; Leichman, L.; Brindle, J.; Vaitkevicius, V.; Cooper, J.; Byhardt, R.; Davis, L. and Emami, B. Combined Chemotherapy and Radiotherapy Compared with Radiotherapy Alone in Patients with Cancer of the Esophagus. *N. Engl. J. Med.* **1992**, *326*, 1593-1598.
5. Monsuez, J. J.; Charniot, J. C.; Vignat, N. and Artigou, J. Y. Cardiac side-effects of cancer chemotherapy. *Int. J. Cardiol.* **2010**, *144*, 3-15.
6. Chabner, B. A. and Roberts, T. G. Chemotherapy and the war on cancer. *Nat. Rev. Cancer* **2005**, *5*, 65-72.
7. Goss, P. E. and Chambers, A. F. Does tumour dormancy offer a therapeutic target? *Nat. Rev. Cancer* **2010**, *10*, 871-877.
8. Lammers, T.; Kiessling, F.; Hennink, W. E. and Storm, G. Drug targeting to tumors: Principles, pitfalls and (pre-) clinical progress. *J. Control. Release* **2012**, *161*, 175-187.
9. Wu, X. M.; Sun, X. R.; Guo, Z. Q.; Tang, J. B.; Shen, Y. Q.; James, T. D.; Tian, H. and Zhu, W. H. In Vivo and in Situ Tracking Cancer Chemotherapy by Highly Photostable NIR Fluorescent Theranostic Prodrug. *J. Am. Chem. Soc.* **2014**, *136*, 3579-3588.

10. Wang, H.; Tang, L.; Tu, C. L.; Song, Z. Y.; Yin, Q.; Yin, L. C.; Zhang, Z. H. and Cheng, J. J. Redox-Responsive, Core-Cross-Linked Micelles Capable of On-Demand, Concurrent Drug Release and Structure Disassembly. *Biomacromolecules* **2013**, *14*, 3706-3712.
11. Fan, J. Q.; Fang, G.; Zeng, F.; Wang, X. D. and Wu, S. Z. Water-Dispersible Fullerene Aggregates as a Targeted Anticancer Prodrug with both Chemo- and Photodynamic Therapeutic Actions. *Small* **2013**, *9*, 613-621.
12. Fan, J. Q.; Zeng, F.; Wu, S. Z. and Wang, X. D. Polymer micelle with pH-triggered hydrophobic–hydrophilic transition and de-cross-linking process in the core and its application for targeted anticancer drug delivery. *Biomacromolecules* **2012**, *13*, 4126-4137.
13. Kim, E. J.; Bhuniya, S.; Lee, H.; Kim, H. M.; Cheong, C.; Maiti, S.; Hong, K. S. and Kim, J. S. An Activatable Prodrug for the Treatment of Metastatic Tumors. *J. Am. Chem. Soc.* **2014**, *136*, 13888-13894.
14. Yuan, Y. Y.; Chen, Y. L.; Tang, B. Z. and Liu, B. A targeted theranostic platinum (IV) prodrug containing a luminogen with aggregation-induced emission (AIE) characteristics for in situ monitoring of drug activation. *Chem. Commun*. **2014**, *50*, 3868-3870.
15. Hu, X. L.; Hu, J. M.; Tian, J.; Ge, Z. S.; Zhang, G. Y.; Luo, K. F. and Liu, S. Y. Polyprodrug amphiphiles: hierarchical assemblies for shape-regulated cellular internalization, trafficking, and drug delivery. *J. Am. Chem. Soc.* **2013**, *135*, 17617-17629.
16. Biswas, S.; Das, J.; Barman, S.; Pinninti, B. R.; Maiti, T. K. and Singh, N. D. P. Environment Activatable Nanoprodrug: Two-Step Surveillance in the Anticancer Drug Release. *ACS Appl. Mater. Interfaces* **2017**, *9*, 28180-28184.
17. Wang, J. Q.; Sun, X. R.; Mao, W. W.; Sun, W. L.; Tang, J. B.; Sui, M. H.; Shen, Y. Q. and Gu, Z. W. Tumor redox heterogeneity‐responsive prodrug nanocapsules for cancer chemotherapy. *Adv. Mater.* **2013**, *25*, 3670-3676.
18. Weinstain, R.; Segal, E.; Satchi-Fainaro, R. and Shabat, D. Real-time monitoring of drug release. *Chem. Commun.* **2010**, *46*, 553-555.
19. Liu, P. L.; Xu, J. S.; Yan, D. H.; Zhang, P. S.; Zeng, F.; Li, B. W. and Wu, S. Z. A DT-diaphorase responsive theranostic prodrug for diagnosis, drug release monitoring and therapy. *Chem. Commun.* **2015**, *51*, 9567-9570.

20. Sharma, K.; Iyer, A.; Sengupta, K. and Chakrapani, H. INDQ/NO, a bioreductively activated nitric oxide prodrug. *Org. Lett.* **2013**, *15*, 2636-2639.
21. Low, P. S.; Henne, W. A. and Doorneweerd, D. D. Discovery and Development of Folic-Acid-Based Receptor Targeting for Imaging and Therapy of Cancer and Inflammatory Diseases. *Acc. Chem. Res.* **2008**, *41*, 120-129.
22. Liu, Y. J.; Zhu, S. J.; Gu, K. Z.; Guo, Z. Q.; Huang, X. Y.; Wang, M. W.; Amin, H. M.; Zhu, W. H. and Shi, P. GSH-Activated NIR Fluorescent Prodrug for Podophyllotoxin Delivery. *ACS Appl. Mater. Interfaces* **2017**, *8*, 29496-29504.
23. Redy, O.; Shabat, D. Modular theranostic prodrug based on a FRET-activated self-immolative linker. *J. Control. Release* **2012**, *164*, 276-82.
24. Redy-Keisar, O.; Ferber, S.; Satchi-Fainaro, R.; Shabat, D. NIR Fluorogenic Dye as a Modular Platform for Prodrug Assembly: Real-Time in vivo Monitoring of Drug Release. *ChemMedChem*. **2015**, *10*, 999-1007.
25. Li, C. M.; Chen, T.; Ocsoy, I.; Zhu, G. Z.; Yasun, E.; You, M. X.; Wu, C. C.; Zheng, J.; Song, E.; Huang, C. Z. and Tan, W. H. Gold-Coated Fe_3O_4 Nanoroses with Five Unique Functions for Cancer Cell Targeting, Imaging, and Therapy. *Adv. Funct. Mater.* **2014**, *24*, 1772-1780.
26. Liu, H. W.; Hu, X. X.; Li, K.; Liu, Y. C.; Rong, Q. M.; Zhu, L. M.; Yuan, L.; Qu, F. L.; Zhang, X. B. and Tan, W. H. A mitochondrial-targeted prodrug for NIR imaging guided and synergetic NIR photodynamic-chemo cancer therapy. *Chem. Sci.* **2017**, *8*, 7689-7695.
27. Akhter, S.; Ahmad, I.; Ahmad, M. Z.; Ramazani, F.; Singh, A.; Rahman, Z.; Ahmad, F. J.; Storm, G. and Kok, R. J. Nanomedicines as Cancer Therapeutics: Current Status. *Curr. Cancer Drug Tar.* **2013**, *13*, 362-378.
28. Lee, M. H.; Yang, Z.; Lim, C. W.; Lee, Y. H.; Dongbang, S.; Kang, C. and Kim, J. S. Disulfide-Cleavage-Triggered Chemosensors and Their Biological Applications. *Chem. Rev.* **2013**, *113*, 5071-5109.
29. Shi, H.; Kwok, R. T. K.; Liu, J.; Xing, B.; Tang, B. Z. and Liu, B. Real-time monitoring of cell apoptosis and drug screening using fluorescent light-up probe with aggregation-induced emission characteristics. *J. Am. Chem. Soc.* **2012**, *134*, 17972-17981.

30. Shin, W. S.; Han, J. Y.; Verwilst, P.; Kumar, R.; Kim, J. H. and Kim, J. S. Cancer Targeted Enzymatic Theranostic Prodrug: Precise Diagnosis and Chemotherapy. *Bioconjugate Chem*. **2016**, *27*, 1419-1426.
31. He, X.-P.; Zang, Y.; James, T. D.; Li, J. and Chen, G.-R. Probing disease-related proteins with fluorogenic composite materials. *Chem. Soc. Rev.* **2015**, *44*, 4239-4248.
32. Ji, D.-K.; Zhang, Y.; Zang, Y.; Li, J.; Chen, G.-R.; He, X.-P. and Tian, H. Targeted Intracellular Production of Reactive Oxygen Species by a 2D Molybdenum Disulfide Glycosheet. *Adv. Mater.* **2016**, *28*, 9356-9363.
33. He, X.-P.; Tian, H. Lightening Up Membrane Receptors with Fluorescent Molecular Probes and Supramolecular Materials. *Chem.* **2018**, *4*, 246-268.
34. Wang, F. Y.; Zhu, Y.; Zhou, L.; Pan, L.; Cui, Z. F.; Fei, Q.; Luo, S. H.; Pan, Dun.; Huang, Q.; Wang, R.; Zhao, C. C.; Tian, H. and Fan, C. H. Fluorescent In Situ Targeting Probes for Rapid Imaging of Ovarian-Cancer-Specific g-Glutamyltranspeptidase. *Angew. Chem. Int. Ed.* **2015**, *54*, 7349 -7353.
35. Mu, J.; Lin, J.; Huang, P. and Chen, X. Y. Development of endogenous enzyme-responsive nanomaterials for theranostics. *Chem. Soc. Rev.* **2018**, *47*, 5554-5573.
36. Kong, F.; Liang, Z. Y.; Luan, D. R.; Liu, X. J.; Xu, K. H. and Tang, B. A Glutathione (GSH)-Responsive Near-Infrared (NIR) Theranostic Prodrug for Cancer Therapy and Imaging. *Anal. Chem.* **2016**, *88*, 6450-6456.
37. Sedgwick, A. C.; Dou, W. T.; Jiao, J. B.; Wu, L. L.; Williams, G. T.; Jenkins, A. T. A.; Bull, S. D.; Sessler, J. L.; He, X. P. and James, T. D. An ESIPT probe for the ratiometric imaging of peroxynitrite facilitated by binding to Aβ-aggregates. *J. Am. Chem. Soc.* **2018**, *140*, 14267-14271.
38. Wang, R. C.; Dong, K. K.; Xu, G.; Shi, B.; Zhu, T. L.; Shi, P.; Guo, Z. Q.; Zhu, W. H. and Zhao, C. C. A molecular design strategy toward enzyme-activated probes with near-infrared I and II fluorescence for targeted cancer imaging. *Chem. Sci*. **2019**, *10*, 2785-2790.
39. Ye, M. Z.; Wang, X. H.; Tang, J. B.; Guo, Z. Q.; Shen, Y. Q.; Tian, H. and Zhu, W. H. Dual-channel NIR activatable theranostic prodrug for in vivo spatiotemporal tracking thiol-triggered chemotherapy. *Chem. Sci*. **2016**, *7*, 4958-4965.

40. Liu, Z. W.; Song, F. L.; Shi, W. B.; Gurzadya, G.; Yin, H. Y.; Song, B.; Liang, R. and Peng, X. J. Nitroreductase-Activatable Theranostic Molecules with High PDT Efficiency under Mild Hypoxia Based on a TADF Fluorescein Derivative. *ACS Appl. Mater. Interfaces* **2019**, *11*, 15426-15435.
41. Lee, M. H.; Sharma, A.; Chang, M. J.; Lee, J.; Son, S.; Sessler, J. L.; Kang, C. and Kim, J. S. Fluorogenic reaction-based prodrug conjugates as targeted cancer theranostics. *Chem. Soc. Rev.* **2018**, *47*, 28-52.
42. Liu, P. L.; Li, B. W.; Zhan, C. Y.; Zeng, F. and Wu, S. Z. A two-photon-activated prodrug for therapy and drug release monitoring. *J. Mater. Chem. B* **2017**, *5*, 7538-7546.
43. Yuan, Y. Y.; Kwok, R. T. K.; Zhang, R. Y.; Tang, B. Z. and Liu, B. Targeted theranostic prodrugs based on an aggregation-induced emission (AIE) luminogen for real-time dual-drug tracking. *Chem. Commun.* **2014**, *50*, 11465-11468.
44. Huang, H.; Tanaka, H.; Hammock, B. D. and Morisseau, C. Novel and highly sensitive fluorescent assay for leucine aminopeptidases. *Anal. Biochem*. **2009**, *391*, 11-16.
45. Yamazaki, T.; Akada, T.; Niizeki, O.; Suzuki, T.; Miyashita, H. and Sato, Y. Puromycin-insensitive leucyl-specific aminopeptidase (PILSAP) binds and catalyzes PDK1, allowing VEGF-stimulated activation of S6K for endothelial cell proliferation and angiogenesis. *Blood* **2004**, *104*, 2345-2352.
46. Bardawill, C.; Chang, C. Serum Lactic Dehydrogenase, Leucine Aminopeptidase and 5-Nucleotidase Activity. *Can. Med. Assoc. J.* **1963**, *89*, 755-761.
47. Reichling, J. J. and Kaplan, M. M. Clinical use of serum enzymes in liver disease. *Dig. Dis. Sci.* **1988**, *33*, 1601-1614.
48. Zhou, Z.; Wang, F. Y.; Yang, G. C.; Lu, C. F.; Nie, J. Q.; Chen, Z. X.; Ren, J.; Sun, Q.; Zhao, C. C. and Zhu, W. H. A Ratiometric fluorescent probe for monitoring leucine aminopeptidase in living cells and zebrafish model. *Anal. Chem.* **2017**, *89*, 11576-11582.
49. Gong, Q. Y.; Shi, W.; Li, L. H. and Ma, H. M. Leucine aminopeptidase may contribute to the intrinsic resistance of cancer cells toward cisplatin as revealed by an ultrasensitive fluorescent probe. *Chem. Sci.* **2016**, *7*, 788-792.
50. Chai, Y.; Gao, Y. T.; Xiong, H. W.; Lv, W. Q.; Yang, G. C.; Lu, C. F.; Nie, J. Q.; Ma, C.; Chen, Z. X.; Ren, J. and Wang, F. Y. A near-infrared fluorescent probe for monitoring leucine aminopeptidase in living cells. *Analyst* **2019**, *144*, 463-467.

51. Zhang, J. J.; Chai, X. Z.; He, X. P.; Kim, H. J.; Yoon, J. Y. and Tian, H. Fluorogenic probes for disease-relevant enzymes. *Chem. Soc. Rev.* **2019**, *48*, 683-722.
52. Xu, S. A.; Liu, H. W.; Hu, X. X.; Huan, S. Y.; Zhang, J.; Liu, Y. C.; Yuan, L.; Qu, F. L.; Zhang, X. B. and Tan, W. H. Visualization of endoplasmic reticulum aminopeptidase 1 under different redox conditions with a two-photon fluorescent probe. *Anal. Chem.* **2017**, *89*, 7641-7648.
53. Wu, B.; Lin, Y.; Li, B. W.; Zhan, C. Y.; Zeng, F. and Wu, S. Z. Oligo(ethylene glycol)-Functionalized Squaraine Fluorophore as a Near-Infrared-Fluorescent Probe for the In Vivo Detection of Diagnostic Enzymes. *Anal. Chem.* **2018**, *90*, 9359-9365.
54. Gu, K. Z.; Liu, Y. J.; Guo, Z. Q.; Lian, C.; Yan, C. X.; Shi, P.; Tian, H. and Zhu, W. H. In situ ratiometric quantitative tracing of intracellular leucine aminopeptidase activity via an activatable near-infrared fluorescent probe. *ACS Appl. Mater. Interfaces* **2016**, *8*, 26622-26629.
55. Fei, Q.; Zhou, L.; Wang, F. Y.; Shi, B.; Li, C. B.; Wang, R.; Zhao, C. C. Rational construction of probes rendering ratiometric response to the cancer-specific enzyme NQO1. *Dyes Pigments* **2017**, *136*, 846-851.

For TOC only

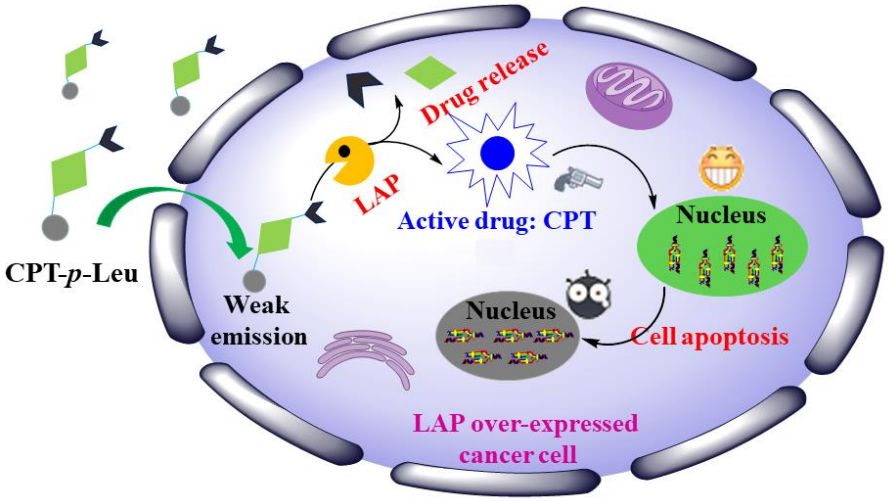
Drug release
LAP
Active drug: CPT
Nucleus
CPT-*p*-Leu
Weak
emission
Nucleus
Cell apoptosis
LAP over-expressed
cancer cell